Plasmons in Sodium under Pressure: Increasing Departure from Nearly Free-Electron Behavior

Plasmons in Sodium under Pressure: Increasing Departure from Nearly Free-Electron Behavior

I. Loa,[1,*] K. Syassen,[1] G. Monaco,[2] G. Vankó,[2,†] M. Krisch,[2] and M. Hanfland[2]

[1]*Max-Planck-Institut für Festkörperforschung, Heisenbergstrasse 1, 70569 Stuttgart, Germany*

[2]*European Synchrotron Radiation Facility, BP 220, 38043 Grenoble Cedex, France*

(Received 21 December 2010; published 16 August 2011)

We have measured plasmon energies in Na under high pressure up to 43 GPa using inelastic x-ray scattering (IXS). The momentum-resolved results show clear deviations, growing with increasing pressure, from the predictions for a nearly free-electron metal. Plasmon energy calculations based on first-principles electronic band structures and a quasiclassical plasmon model allow us to identify a pressure-induced increase in the electron-ion interaction and associated changes in the electronic band structure as the origin of these deviations, rather than effects of exchange and correlation. Additional IXS results obtained for K and Rb are addressed briefly.

DOI: 10.1103/PhysRevLett.107.086402 PACS numbers: 71.45.Gm, 62.50.−p, 71.20.−b, 78.70.Ck

Sodium, at ambient conditions, is one of the best manifestations of a "simple" or nearly free-electron (NFE) metal [1]. It is characterized by a single *s*-type valence electron, weak interaction between the conduction electrons and the atomic cores (electron-ion interaction), and conduction band states of *sp* orbital character. Na crystallizes in the high-symmetry body-centered cubic (bcc) structure at pressures up to 65 GPa, where it transforms to face-centered cubic (fcc) [2]. The properties of Na change fundamentally under pressure in the megabar pressure range, where a series of phase transitions into lower-symmetry crystal structures has been predicted [3] and observed [4–6], accompanied by marked changes in its optical properties [4,6,7] and culminating in the formation of a nonmetallic, visually transparent phase at ~200 GPa [8]. A central question is how the transformation from a simple metal to a semiconductor progresses, not only in Na, but also in other metals such as Li, which was reported to become semiconducting above 70 GPa [9]. As for Na, does it remain NFE-like in its bcc and fcc phases up to ~100 GPa [7] so that the non-NFE behavior starts only with the transitions into the lower-symmetry phases above 105 GPa, or are there significant precursors at lower pressure?

To provide an answer, we measured and calculated the pressure dependence of Na plasmon energies. Plasmon excitations provide information on the collective electronic excitations in the form of longitudinal charge density waves at finite wave vector, and they determine the optical response of a metal, specifically the plasma reflection edge. Plasmons have been studied for many years by electron-energy-loss spectroscopy (EELS) at zero pressure (see, for example, [10,11] and references therein), but this technique is not suitable for samples enclosed in high-pressure cells. Mao *et al.* [12] have demonstrated the possibility of measuring plasmon excitations in Na under pressure using inelastic x-ray scattering (IXS), and they found their experimental results up to 2.7 GPa to be in agreement with theoretical predictions.

We report here detailed IXS results on the plasmon energy dispersion in Na under pressure up to 43 GPa, corresponding to a 2.6-fold increase in density. Our results evidence a significant departure from the predictions for a NFE metal. In order to explain this discrepancy between theory and experiment, we also present plasmon energy calculations based on first-principles electronic band structures and a quasiclassical plasmon model after Paasch and Grigoryan (PG model) [13]. These calculations reconcile experiment and theory and allow us to identify changes in the electron-ion interaction as the dominant effect, rather than changes in the electron-electron interactions. Some experimental results are also reported for K and Rb.

The theoretical description of plasmons in simple metals is well established. The most commonly used approach starts from the free-electron (FE) gas and uses the random phase approximation (RPA) [14]. The plasmon energy dispersion $E_p(q)$ is then given by $E_p(q) = \hbar\omega_p + \frac{\hbar^2}{m}\alpha q^2$ with the plasma frequency $\omega_p = \sqrt{ne^2/\epsilon_0\epsilon_s m}$ and the dispersion coefficient $\alpha_{\mathrm{FE}} = \frac{3}{5}E_F/\hbar\omega_p$, where q is the plasmon momentum, m the electron mass, n the electron density, ϵ_s a dielectric constant describing the polarizability of the ionic cores ($\epsilon_s = 1$ for the free-electron gas), and $E_F = (\hbar^2/2m)(3\pi^2 n)^{2/3}$ is the Fermi energy. This relatively simple model works reasonably well for simple metals such as Na and Al at ambient conditions [10,11], but experimental dispersion coefficients α tend to be lower than the theoretical values, which has been attributed to electron exchange and correlation effects [11]. Both the plasma frequency ω_p and the dispersion coefficient α depend on the electron density and can thus be tuned by the application of pressure; both are expected to increase with increasing pressure. The stability of bcc sodium over a large pressure range of 0–65 GPa permits us to generate an up to threefold increase in (electron) density without a structural transition.

IXS experiments were performed on beam line ID16 at the ESRF, Grenoble. Silicon crystal monochromators were used to monochromatize the incident beam and to analyze the scattered radiation. The incident x-ray beam with a photon energy of 9.877 keV was focused onto the polycrystalline sample in a high-pressure cell with a spot diameter of 100–200 μm, depending on the sample size. IXS spectra of the samples at room temperature were recorded in energy-scanning mode with an overall spectral resolution of 0.6 eV and a momentum resolution of 0.4 nm^{-1}. In most of the experiments, the samples were pressurized in diamond anvil cells (DACs). Rhenium and stainless steel gaskets were used with initial thicknesses of 50–100 μm and hole diameters of 150–200 μm. The loading of distilled Na, K, and Rb into the pressure cells was carried out in an argon atmosphere. Because of the softness of these metals no pressure transmitting medium was added. Pressures were determined with the ruby method [15] or by measuring an x-ray powder diffraction of the sample and using its known equation of state [2]. In the experiments using a DAC, the incoming x-ray beam passed through one diamond anvil onto the sample, and the scattered radiation was collected through the opposing anvil (thickness ~1.5 mm). Despite the small sample scattering volume and the relatively low diamond transmittance of 30% for 10-keV x rays, high-quality spectra could be collected in ~2 h. The experiments on Na at 1 and 7 GPa were performed using a high-pressure cell equipped with sintered-diamond anvils and a beryllium gasket. Here, the x rays passed through the Be gasket.

Figure 1 shows IXS spectra of polycrystalline Na under pressure. A single excitation peak is observed, which is attributed to the bulk plasmon in Na, based on the predictions for a NFE metal with the electron density of Na and also by comparison with previous EELS results [10]. The rising background in the spectra of Fig. 1, particularly at large q, is due to plasmon and interband excitations in the diamond anvil through which the scattered radiation is detected [16].

Plasmon energies and linewidths were determined by fitting the spectra with a Gaussian peak for the plasmon line and a polynomial background. As all experiments were performed on polycrystalline samples, the reported plasmon energies are directional averages. The Na plasmon energies increase with increasing pressure as illustrated in Fig. 2 for $q = 5$ nm^{-1}. This is in *qualitative* agreement with the NFE picture, where the plasmon energies scale with the electron density.

Figure 2 also shows results for K and Rb. These two metals clearly do not follow the expectations for NFE metals. Moreover, their plasmon linewidths increased and their plasmon intensities decreased rapidly with increasing pressure. These effects are attributed to the pressure-driven s-d hybridization of conduction band states, as is also evident from the optical response of K and Rb under pressure [17,18] (see also [19]). We will therefore focus on Na that could be studied over the largest pressure range and which, at ambient conditions, is one of the best manifestations of a nearly free-electron metal.

Figure 3(a) shows the measured plasmon dispersion relations of Na at several pressures. The plasmon energies are plotted versus q^2 because of the anticipated parabolic dispersion relation, see the $E_p(q)$ relation given above. At the lowest pressure, 1 GPa, the Na plasmon dispersion measured here is indeed very close to parabolic. Results of an ambient-pressure EELS study [10] are included in Fig. 3(a) for comparison. In the low-q region, the IXS and EELS data are reasonably consistent, but the EELS results exhibit some deviation from a parabolic dispersion. The offset, at low q, between the IXS and EELS data is largely due to the pressure applied in the IXS experiment. The 1-GPa plasmon dispersion measured by IXS is described

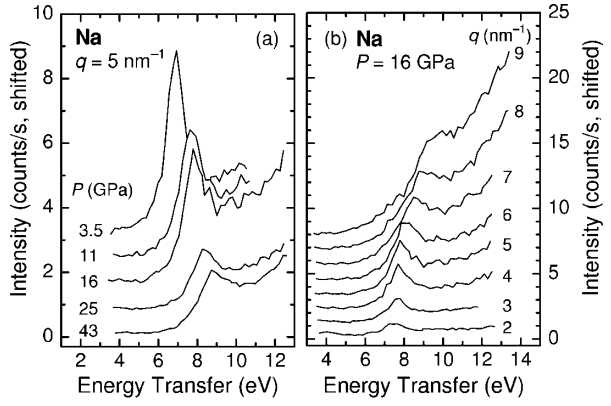

FIG. 1. IXS spectra of polycrystalline sodium pressurized in a diamond anvil cell. (a) Energy transfer spectra for a momentum transfer of $q = 5$ nm^{-1} and pressures of 3.5–43 GPa. (b) Energy transfer spectra of Na at 16 GPa and momentum transfers of 2–9 nm^{-1}. Vertical offsets are added for clarity.

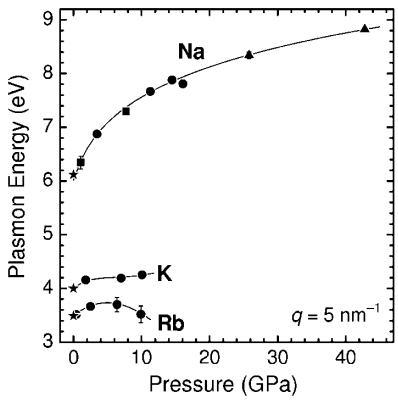

FIG. 2. Plasmon energies in Na, K, and Rb at $q = 5$ nm^{-1} as a function of pressure. Ambient-pressure EELS results [10] are indicated by stars. For the Na data, different symbols distinguish different sample loadings and pressure cells. Lines are guides to the eye.

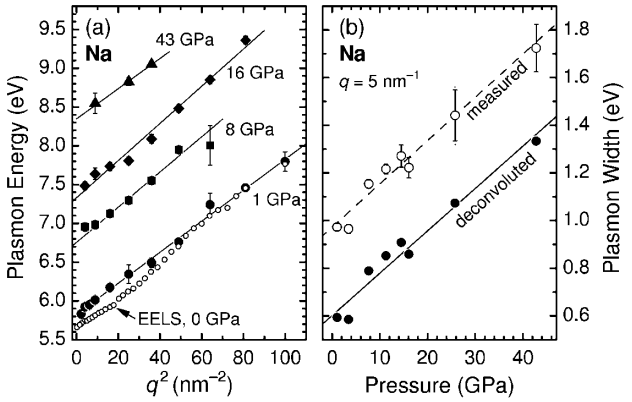

FIG. 3. (a) Plasmon dispersions $E(q^2)$ of polycrystalline Na as a function of pressure. Ambient-pressure electron-energy-loss spectroscopy results by vom Felde *et al.* [10] are indicated by small open symbols. (b) Plasmon linewidth of Na versus pressure.

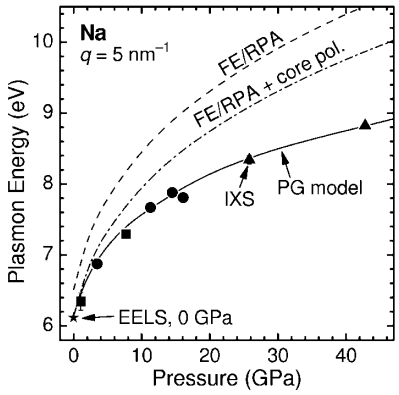

FIG. 4. Experimental pressure dependence of the directionally averaged plasmon energy in Na at $q = 5$ nm^{-1} (large symbols) and results of the free-electron (FE) gas model, FE model with core polarization, and the PG model (solid line). The star indicates the ambient-pressure EELS result [10].

best by $E(0) = \hbar\omega_p = 5.82(2)$ eV and $\alpha = 0.26(1)$. As noted before [10], the experimental dispersion parameter α is lower than the FE/RPA value of $\alpha_{\mathrm{RPA}} = 0.35$. Towards higher pressures, the measured plasmon dispersion remains approximately parabolic, deviations being most notable at 16 GPa.

Figure 3(b) shows that also the plasmon linewidth is strongly pressure dependent. This effect is tentatively attributed to a reduction of the plasmon lifetime due to decays involving electron-hole excitations. A detailed study by, e.g., time-dependent density functional theory could be a subject for future studies. For the remainder of this Letter we focus on the plasmon energies, assuming that self-energy effects on the plasmon frequency can be neglected.

The IXS results on the plasmon energies of Na as a function of momentum and pressure allow us to test the validity of the FE/RPA description of Na and to assess the relative importance of band-structure effects, core polarizability, and exchange and correlation. Using $E_p(q)$ as given above and the experimental equation of state of Na [2], the pressure dependence of the $q = 5$ nm^{-1} plasmon was calculated within the FE/RPA framework as shown in Fig. 4. This FE/RPA estimate is significantly higher in energy than the experimental values, and the deviation increases with increasing pressure. Inclusion of the core polarization ($\epsilon_s = 1.16$, Ref. [20]) leads to a good agreement with the experiment at low pressure, but a major deviation between theory and experiment remains at high pressure.

The important observation here is the striking increase in the deviation between theory and experiment with increasing pressure. In previous work on other metals, deviations from the FE/RPA predictions were discussed in relation to exchange and correlation effects [10,21], and a number of extensions of the RPA were proposed in this spirit (see [10,21,22] and references therein). Their main effect is to reduce the plasmon dispersion coefficient α, and their inclusion can improve the agreement between theory and experiment. However, exchange-correlation effects decrease with increasing electron density, and they can thus be excluded as the origin of the deviation between the "FE/RPA + core polarization" results and the experimental data in Fig. 4. More recent theoretical studies have emphasized the importance of band-structure effects on the plasmon properties, regarding both the energy dispersion [13] and the plasmon linewidth [19]. The present IXS results offer an opportunity to test these proposals.

The PG plasmon model [13] adopted here is an extension of the FE/RPA approach. This classical model is not expected to describe the plasmon properties as accurately as, e.g., time-dependent density functional theory (DFT) [19], but it allows us better to understand the underlying physics. The electronic structure of the metal is described here by a single isotropic conduction band with a quartic dispersion, $E(k) = E_2k^2 + E_4k^4$. The E_4k^4 term accounts for deviations from the parabolic band shape of the free-electron gas. The plasma frequency ω_p and the plasmon dispersion coefficient α can then be determined from E_2, E_4 and the Fermi energy E_F as described in detail in [13].

Electronic structure calculations of Na were performed in the framework of first-principles DFT, using the full-potential L/APW + lo method [23,24] and the generalized gradient approximation [25] as implemented in the WIEN2K code [26]. The electronic band structure of bcc Na was calculated for a series of volumes corresponding to the pressure range of 0–50 GPa [27]. The coefficients E_2 and E_4 were determined for three directions in the Brillouin zone, i.e., along $[\xi 00]$, $[\xi\xi 0]$, and $[\xi\xi\xi]$, and then averaged [28]. The only adjustable parameter in the calculation of the plasma frequency and the dispersion coefficient is the static dielectric constant ϵ_s that accounts for the polarizability of the ionic cores. A value of $\epsilon_s = 1.16$ as determined for Na in a DFT-based study [20] was adopted here, and a possible density dependence was neglected.

TABLE I. Experimental plasma frequencies ω_p and dispersion coefficients α of Na as a function of pressure and comparison with theoretical results. The experimental values were determined from linear fits to the $E(q^2)$ data as shown in Fig. 3(a).

	Experiment		FE/RPA		PG model	
P (GPa)	$\hbar\omega_p$ (eV)	α	$\hbar\omega_p$ (eV)	α	$\hbar\omega_p$ (eV)	α
1.0	5.82(2)	0.26(1)	5.84	0.35	5.82	0.31
7.7	6.8(1)	0.26(2)	6.99	0.37	6.77	0.31
16.1	7.3(1)	0.32(2)	7.74	0.39	7.35	0.29
42.8	8.3(1)	0.26(2)	9.10	0.41	8.33	0.26

Figure 4 shows the results of the PG model with input from our band-structure calculations for the $q = 5$ nm^{-1} plasmon in Na [28]. The computed results are in excellent agreement with the IXS data. To trace the source of the difference between the FE/RPA results and those of the PG model, Table I summarizes the plasma frequency $\hbar\omega_p$ and the dispersion coefficient α for the two models at selected pressures. At 1 GPa, the results of the NFE/RPA and the PG model are very similar, and the calculated plasma frequency agrees well with the experiment. As noted before [10], the calculated values of α are 20%–30% larger than in the experiment, and this is probably due to exchange-correlation effects not included here. The effect of the nonparabolic contribution ($E_4 < 0$) is to reduce both $\hbar\omega_p$ and α. In Na, this effect is very small near ambient pressure, confirming the analysis by Paasch and Grigoryan [13]. With increasing pressure, however, $|E_4|$ increases and leads to substantial corrections [28]. At 40 GPa, it reduces the plasma frequency by 8% and the dispersion coefficient by 35% compared to NFE/RPA. Table I also shows that α *decreases* with increasing pressure in the PG model, in contrast to the free-electron behavior. We would like to emphasize that it is the nonparabolic contribution that causes the renormalization of the plasmon energies, even though the corrections to the band energies are less than 3% of the band width [28].

As for the physical origin of these corrections, the band-structure calculations show that pressure causes the band gaps at the N, P, and H points of the Brillouin zone to grow relative to the width of the conduction band [28]. This evidences a strengthening of the interaction between the valence electrons and the ionic cores (electron-ion interaction). In other words, Na becomes increasingly less free-electron-like under compression. The quartic correction ($E_4 < 0$) corresponds to a lowering of the conduction band energies near the Brillouin zone boundary in comparison to the free-electron case, and this distortion of the band structure [28] leads to a reduction of the Fermi velocity, $v_F = (1/\hbar)\partial E(k)/\partial k|_{k_F} = (2k_F/\hbar)(E_2 + 2E_4 k_F^2)$, which is the key physical quantity that determines the plasmon dispersion.

In summary, we have performed inelastic x-ray scattering experiments to determine the effect of pressure on the plasmon excitations in the "simple metal" sodium. While Na is considered one of the best manifestations of a nearly free-electron metal at ambient conditions, our results evidence substantial and increasing deviations from the behavior of a NFE metal at high pressure up to 43 GPa. This can be seen as an early precursor of the fundamental changes in the electronic structure of Na at megabar pressures. The deviation from NFE behavior can in part be attributed to the polarizability of the ionic cores, but to a larger extent it is caused by pressure-induced changes in the electronic band structure. Plasmon energies determined on the basis of electronic band-structure calculations and the quasiclassical PG model are in excellent agreement with the IXS results. They show that the electron-ion interaction in Na increases with pressure and leads to the renormalization of the plasmon energies via a modification of the electronic band structure. As for the heavy alkali metals under pressure, band-structure effects can be expected to be even more important due to the pressure-driven hybridization of the valence s orbitals with d states, as discussed before [13]. We observed a weak pressure dependence of the plasmon frequencies of K and Rb combined with fast broadening of their plasmon resonances under pressure. These results may aid the interpretation of plasmon dispersions of the heavy alkali metals at ambient pressure. As for bulk Li metal, the quite detailed predictions on the collective electronic response under pressure [29,30] still await a related experimental investigation.

We thank F. Kögel (MPI-FKF, Stuttgart) for providing the distilled metals used in this study. G. V. was supported by the Hungarian Scientific Research Fund (Contract No. K72597).

*Corresponding author.
I.Loa@ed.ac.uk
Present address: SUPA, School of Physics and Astronomy, Centre for Science at Extreme Conditions, The University of Edinburgh, U.K.
†Present address: KFKI Research Institute for Particle and Nuclear Physics, P.O. Box 49, H-1525 Budapest, Hungary.

[1] E. Wigner and F. Seitz, Phys. Rev. **46**, 509 (1934).
[2] M. Hanfland, I. Loa, and K. Syassen, Phys. Rev. B **65**, 184109 (2002).
[3] J. B. Neaton and N. W. Ashcroft, Phys. Rev. Lett. **86**, 2830 (2001); N. E. Christensen and D. L. Novikov, Solid State Commun. **119**, 477 (2001).
[4] M. Hanfland *et al.*, "Sodium at Megabar Pressures," in High Pressure Gordon Conference 2002 (unpublished).
[5] E. Gregoryanz *et al.*, Science **320**, 1054 (2008).
[6] L. F. Lundegaard *et al.*, Phys. Rev. B **79**, 064105 (2009).
[7] A. Lazicki *et al.*, Proc. Natl. Acad. Sci. U.S.A. **106**, 6525 (2009).
[8] Y. Ma *et al.*, Nature (London) **458**, 182 (2009).
[9] T. Matsuoka and K. Shimizu, Nature (London) **458**, 186 (2009).

[10] A. vom Felde, J. Sprösser-Prou, and J. Fink, Phys. Rev. B **40**, 10 181 (1989).
[11] J. Sprösser-Prou, A. vom Felde, and J. Fink, Phys. Rev. B **40**, 5799 (1989).
[12] H.-K. Mao, C. Kao, and R. J. Hemley, J. Phys. Condens. Matter **13**, 7847 (2001).
[13] G. Paasch and V. G. Grigoryan, Ukr. J. Phys. **44**, 1480 (1999).
[14] D. Pines, *Elementary Excitations in Solids* (W. A. Benjamin, New York, 1964).
[15] G. J. Piermarini, S. Block, J. D. Barnett, and R. A. Forman, J. Appl. Phys. **46**, 2774 (1975); H. K. Mao, J. Xu, and P. M. Bell, J. Geophys. Res. **91**, 4673 (1986).
[16] S. Waidmann *et al.*, Phys. Rev. B **61**, 10 149 (2000).
[17] H. Tups, K. Takemura, and K. Syassen, Phys. Rev. Lett. **49**, 1776 (1982).
[18] K. Takemura and K. Syassen, Phys. Rev. B **28**, 1193 (1983).
[19] W. Ku and A. G. Eguiluz, Phys. Rev. Lett. **82**, 2350 (1999).
[20] R. Nieminen and M. Puska, Phys. Scr. **25**, 952 (1982).
[21] L. Serra *et al.*, Phys. Rev. B **44**, 1492 (1991).
[22] P. Vashishta and K. S. Singwi, Phys. Rev. B **6**, 875 (1972).
[23] E. Sjösted, L. Nordström, and D. J. Singh, Solid State Commun. **114**, 15 (2000).
[24] G. K. H. Madsen *et al.*, Phys. Rev. B **64**, 195134 (2001).
[25] J. P. Perdew, K. Burke, and M. Ernzerhof, Phys. Rev. Lett. **77**, 3865 (1996).
[26] P. Blaha *et al.*, *WIEN2k, An Augmented Plane Wave + Local Orbitals Program for Calculating Crystal Properties* (K. Schwarz, Techn. Universität Wien, Austria, 2001).
[27] Computational details: sphere size $R_{\mathrm{MT}} = 2.0$ a.u.; plane-wave cutoff defined by $R_{\mathrm{MT}} \times \max(k_n) = 8.0$; Brillouin zone sampled on a tetrahedral mesh with 18^3 k points (190 in the IBZ).
[28] See Supplemental Material at http://link.aps.org/supplemental/10.1103/PhysRevLett.107.086402 for additional details and results of the electronic-structure calculations.
[29] A. Rodriguez-Prieto, V. M. Silkin, A. Bergara, and P. M. Echenique, New J. Phys. **10**, 053035 (2008).
[30] I. Errea *et al.*, Phys. Rev. B **81**, 205105 (2010).